Preparation, Characterization, and the Crystal Structure of the Inhibitor ZK-807834 (CI-1031) Complexed with Factor Xa[†,‡]

Marc Adler,[§] David D. Davey,[§] Gary B. Phillips,[§] Sung-Hou Kim,[||] Jarmila Jancarik,[||] Galina Rumennik,[§] David R. Light,[§] and Marc Whitlow*[,§]

Berlex Biosciences, 15049 San Pablo Avenue, P.O. Box 4099, Richmond, California 94804-0099, and Department of Chemistry and Lawrence Berkeley National Laboratory, University of California Berkeley, California 94720-5230

Received June 27, 2000

ABSTRACT: Factor Xa plays a critical role in the formation of blood clots. This serine protease catalyzes the conversion of prothrombin to thrombin, the first joint step that links the intrinsic and extrinsic coagulation pathways. There is considerable interest in the development of factor Xa inhibitors for the intervention in thrombic diseases. This paper presents the structure of the inhibitor ZK-807834, also known as CI-1031, bound to factor Xa and provides the details of the protein purification and crystallization. Results from mass spectrometry indicate that the factor Xa underwent autolysis during crystallization and the first EGF-like domain was cleaved from the protein. The crystal structure of the complex shows that the amidine of ZK-807834 forms a salt bridge with Asp189 in the S1 pocket and the basic imidazoline fits snugly into the S4 site. The central pyridine ring provides a fairly rigid linker between these groups. This rigidity helps minimize entropic losses during binding. In addition, the structure reveals new interactions that were not found in the previous factor Xa/inhibitor complexes. ZK-807834 forms a strong hydrogen bond between an ionized 2-hydroxy group and Ser195 of factor Xa. There is also an aromatic ring-stacking interaction between the inhibitor and Trp215 in the S4 pocket. These interactions contribute to both the potency of this compound (K_I = 0.11 nM) and the >2500-fold selectivity against homologous serine proteases such as trypsin.

Malfunctions of the blood coagulation cascade can lead to life-threatening conditions such as deep vein thrombosis. Selective factor Xa inhibitors hold the promise of achieving greater antithrombotic efficacy with lower bleeding risk (wider therapeutic index) compared to currently used anticoagulant drugs for treatment and long-term prevention of thrombosis. Factor Xa, a trypsin-like serine protease, catalyzes the proteolytic activation of thrombin at the convergence of the intrinsic and extrinsic pathways and initiates the final common pathway in the blood coagulation cascade (*1*, *2*). This primary activity of factor Xa is enhanced several 1000-fold when factor Xa combines with the cofactor, factor Va, and calcium on the platelet phospholipid membrane surface to form the prothrombinase complex (*3*). Ex vivo data show that this prothrombinase complex, not thrombin, is responsible for the major procoagulant activity on human whole-blood clots. This suggests that factor Xa may be a more important mediator of thrombus progression than thrombin (*4*, *5*). In addition to this essential role in the formation of the prothrombinase complex, free factor Xa plays an important role in the intrinsic coagulation pathway by converting factors V and VIII to their active forms (*6*). Experiments performed with the factor Xa inhibitor tick anticoagulant protein (TAP) in a dog thrombolytic model indicated that a selective factor Xa inhibitor is efficacious with less perturbation of haemostasis than the thrombin inhibitor hirudin (*7*). These studies indicate that an inhibitor of factor Xa would offer an important new tool in the treatment of thrombotic diseases.

Selectivity is a key issue in the design of small molecule inhibitors of serine proteases. Nature uses serine proteases in a variety of biological pathways. These proteases show significant structural homology to factor Xa and many share factor Xa's preference for binding a basic amino acid in the S1 pocket. The S1 pocket binds the residue that precedes the proteolytic cleavage site of the substrate. Most serine protease inhibitors discovered thus far have strong interactions in this pocket. Trypsin, an important digestive enzyme, shares this preference for binding either arginine or lysine in the S1 pocket. X-ray crystallographic studies indicate that the structure of the S1 pocket is nearly identical in both proteins (*8*−*12*).

The S4 pocket also plays an important role in the binding of factor Xa inhibitors. The three published structures of factor Xa/inhibitor complexes all show a positively charged moiety in the S4 site (*8*−*10*). Unfortunately, trypsin binds positive charges in this site as well (*11*, *12*) and many factor Xa inhibitors cross-react with trypsin (*13*, *14*).

[†] The X-ray diffraction data was collected at the Stanford Synchrotron Radiation Laboratory, which is funded by the Department of Energy (BES, BER) and the National Institutes of Health (NCRR, NIGMS).

[‡] The atomic coordinates described in this paper have been deposited with the Protein Data Bank (entry 1FJS).

* To whom correspondence should be addressed. E-mail: marc_whitlow@berlex.com. Fax: (510) 262-7844. Phone: (510) 669-4575.

[§] Berlex Biosciences.

[||] Department of Chemistry and Lawrence Berkeley National Laboratory.

10.1021/bi001477q CCC: $19.00
Published on Web 09/19/2000

We have developed a novel factor Xa inhibitor that is a promising clinical candidate, ZK-807834[1] (also referred to as CI-1031). This compound is a potent inhibitor of factor Xa (K_I = 0.11 nM) and shows >2500-fold selectivity for factor Xa versus trypsin and higher selectivity verses other blood coagulation cofactors (*13*, *14*). Recent experiments have shown that ZK-807834 is effective in rabbit models of both venous and arterial thrombosis (*15*). The results indicate that ZK-807834 is active at lower doses and may cause less perturbation of systemic homeostasis when compared to other available antithrombotic agents. This article describes in detail the preparation and characterization of des-GLA-factor Xaβ used in these studies and the conditions used for crystallization of the factor Xa/ZK-807834 complex. The crystal structure itself provides important information for the design of potent selective serine protease inhibitors.

EXPERIMENTAL PROCEDURES

Compound Synthesis. The synthesis and structure activity relationships of *N*-[2-[5-[amino(imino)methyl]-2-hydroxyphenoxy]-3,5-difluoro-6-[3-(4,5-dihydro-1-methyl-1*H*-imidazol-2-yl)phenoxy]pyridin-4-yl]-*N*-methylglycine (ZK-807834) and related compounds have been described previously (*13*, *14*).

Inhibition Constants (K_I) for Factor Xa and Trypsin. Commercial-purified serine proteases, human factor Xa (Enzyme Research Laboratories, Inc., South Bend, IN) and bovine cationic trypsin (Roche Diagnostics Corp., Indianapolis, IN), were assayed with Chromogenix substrates, catalog numbers S-2222 and S-2266 (Diapharma Group Inc., West Chester, OH). Assays were performed in 150 mM NaCl, 2.5 mM $CaCl_2$, 50 mM Tris-HCl, pH 7.5, and 0.1% PEG 6000 in a final volume of 200 μL in 96-well microtiter plates at room temperature. The initial rate of substrate cleavage by the enzyme was determined by measuring the increases in absorbance at 405 nm with a ThermoMax microplate reader (Molecular Devices Corp., Sunnyvale, CA). Final concentrations of enzyme and substrate were 1 nM factor Xa with 164 μM S-2222, and 16 nM trypsin with 127 μM S-2266. Data were analyzed as previously descried (*13*).

Preparation of Des-GLA-Factor Xaβ. Des-GLA-factor Xaβ was prepared by partial chymotrypsin digestion (*8*, *9*) as follows. Approximately 4 mg of factor Xaβ (Enzyme Research Lab., South Bend, IN) was desalted into 50 mM Tris, pH 8.0. The factor Xaβ was then treated for 1.5 h at 22 °C with sequencing grade chymotrypsin (Boehringer Mannhein, Germany) at a 1:200 molar ratio while shaking in a water bath. During optimization of this protocol, the best results were obtained for this digestion in the absence of factor Xa inhibitors, such as benzamidine. The chymotrypsin inhibitor L-1-chloro-3-(4-tosylamido)-4-phenyl-2-butanone (TPCK; Boehringer Mannhein, Germany) was added in 1000-fold molar excess to stop the digestion. The partially digested factor Xaβ was passed through a 0.22 μm filter. The des-GLA-factor Xaβ was purified on a MonoQ HR 5/5 anion exchange column (Amersham Pharmacia Biotech, Piscataway, NJ). It was eluted with a NaCl gradient buffered with 50 mM TRIS, pH 8.0. Fractions B1 and B2 (Figure 1) eluted with approximately 75 mM NaCl. These fractions were pooled together and were found to contain approximately 0.3 mg of des-GLA-factor Xaβ.

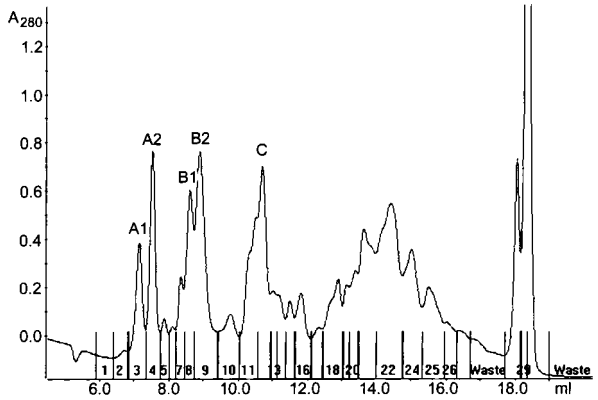

FIGURE 1: Chromatogram of the des-GLA-factor Xaβ purification by anion exchange chromatography on a MonoQ HR 5/5 anion exchange column after chymotrypsin treatment.

Mass Spectrometry Analysis. The molecular masses of the des-GLA-factor Xaβ fractions were determined by mass spectrometry on a Finnigan LCQ with electrospray ionization (Finnigan Inc., San Jose, CA). The des-GLA-factor Xaβ samples were dialyzed overnight against 0.1% acetic acid using 10 000 MW cutoff dialysis cassettes (Pierce Inc., Rockford, IL). They were then concentrated to 0.3−1.0 mg/mL using centrifugal microconcentrators (Amicon Inc., Bedford, MA). In addition, a factor Xa/ZK-807834 crystal was dissolved in 50 μL of 0.1% acetic acid and then dialyzed against 0.1% acetic acid overnight. Prior to analysis, 10 μL of 0.1% acetic acid in methanol was added to an equal volume of the protein samples. A total of 2 μL from each sample was then injected into the Finnigan LCQ using a micro HPLC column (Utlrafast Microprotein Analyzer, Michrom BioResources Inc., Auburn, CA). The samples were introduced into the Finnigan LCQ at 50 μL/min isocratic flow of 95% acetonitrile, 0.1% acetic acid, and 0.005% heptafluorobutyric acid. The LCQ settings were as follows: spray voltage 4.8 kV, capillary voltage 39 V, capillary temperature 210 °C, CID off, and scan range 150−2000 Amu.

Isoelectric Point Determinations. The isoelectric points of the des-GLA-factor Xaβ fractions were determine by capillary electrophoresis on a Beckman P/ACE system 5000 using the eCAP cIEF 3-10 kit (Beckman Instruments Inc., Fullerton, CA). The des-GLA-factor Xaβ samples were dialyzed in 0.1% acetic acid and concentrated to approximately 1 mg/mL as above. A total of 10 μL of a des-GLA-factor Xaβ sample was added to 204 μL of IEFgel with ampholytes, as per the cIEF kit instructions. The des-GLA-factor Xaβ sample-IEFgel-ampholyte solutions were loaded into a 27 cm eCAP neutral capillary using a 1 min high-pressure load

[1] Abbreviations: compound **IV**, 2-[5-[amino(imino)methyl]-2-hydroxyphenoxy]-6-[3-(4,5-dihydro-1H-imidazol-2-yl)phenoxy]pyridine-4-carboxylic acid; compound **V**, 1-[2-[5-[amino(imino)methyl]-2-hydroxyphenoxy]-3,5-difluoro-6-[3-(4,5-dihydro-1-methyl-1*H*-imidazol-2-yl)phenoxy]pyridin-4-yl]piperidine-3-carboxylic acid; EGF epidermal growth factor; des-GLA-factor Xaβ, a factor Xa construct with the EGF 1 and 2 domains, and the serine protease domain; DX-9065a, (2S)-{4-[1-acetimidoyl-(3S)-pyrrolidinyl]-oxyphenyl}-3-(7-amidino-2-naphthyl) propionic acid; FX-2212a, (2*S*)-(3′-amidino-3-biphenyl)-5-(4-pyridylamino)pentanoic acid; TRIS, tris-(hydroxymethyl)aminomethane; ZK-807834, *N*-[2-[5-[amino(imino)methyl]-2-hydroxyphenoxy]-3,5-difluoro-6-[3-(4,5-dihydro-1-methyl-1*H*-imidazol-2-yl)phenoxy]pyridin-4-yl]-*N*-methylglycine also referred to as CI-1031.

Table 1: Molecular Weight and Isoelectric Point Calculations[a]

protein (with C-termini)	molecular weight calcd	molecular weight obsd	isoelectric point calcd	isoelectric point obsd	peak
Des-GLA-factorXaβ (**L** + **H**)	36 927		6.15		
L-ERRKR + **H**-TRGLPK	37 762	38 063	7.47	7.74	A1
L-ERRKR + **H**-TR	37 367	37 672	7.05	6.91	A2
L-ERRK + **H**-TRGLPK	37 607	37 952	7.05	6.74	B1
L-ERRK + **H**-TR	37 211	37 520	6.66	6.51	B2
L-ERR + **H**-TR	37 083	37 374	6.37	6.15	C
EGF2-ERK + **H**-TRGLPK	32 987	33 243	8.11		dissolved crystal

[a] Where the sequences of L, H and EGF2 are as follows:

```
L ≡        KDGDQC ETSPCQNQGK CKDGLGEYTC TCLEGFEGKN CELFTRKLCS
       LDNGDCDQFC HEEQNSVVCS CARGYTLADN GKACIPTGPY PCGKQTL-ER

EGF2 ≡                                                   KLCS
       LDNGDCDQFC HEEQNSVVCS CARGYTLADN GKACIPTGPY PCGKQTL-ER

H ≡        IVGGQE CKDGECPWQA LLINEENEGF CGGTILSEFY ILTAAHCLYQ
       AKRFKVRVGD RNTEQEEGGE AVHEVEVVIK HNRFTKETYD FDIAVLRLKT
       PITFRMNVAP ACLPERDWAE STLMTQKTGI VSGFGRTHEK GRQSTRLKML
       EVPYVDRNSC KLSSSFIITQ NMFCAGYDTK QEDACQGDSG GPHVTRFKDT
       YFVTGIVSWG EGCARKGKYG IYTKVTAFLK WIDRSMK-TR
```

(20 psi), then focused by applying a 500 V/cm (13.5 kV) electric field. After 2 min, the samples were pushed past the UV detector by applying low pressure (0.5 psi), while maintaining the electric field. After running the des-GLA-factor Xaβ samples alone, four standards were added to each des-GLA-factor Xaβ-IEFgel-ampholyte solution and the isoelectric focusing run was repeated. The four standards were ribonuclaese A (pI 9.45), carbonic anhydrase (pI 5.90), β-lactoglobin A (pI 5.10), and CCK flanking peptide (pI 2.75). The isoelectric points of the des-GLA-factor Xaβ samples were determined from a linear fit to the four standards.

Crystallization of ZK-807834 Des-GLA-Factor Xaβ. Fractions B1 and B2 from anion-exchange purification were used for crystallization. A 3-fold excess of ZK-807834, with 1 equiv of HCl, was added to the des-GLA-factor Xaβ and concentrated to approximately 12 mg/mL. Initial crystallization conditions were identified using Hampton Research's Crystal Screen I (*16*) condition 43 (30% PEG-1500) using 2 μL of complex with 2 μL of reservoir over a 0.5 mL reservoir. The optimized crystallization conditions used a 1 mL reservoir containing 15−21% PEG-1500 and 10 mM $CaCl_2$.

Crystallographic Data Collection. A crystal was transferred from its crystallization drop to a drop containing 15% glycerol, 7.5% (*R*,*R*)-(−)-2,3-butanediol (Sigma, St. Louis, MO), 15.75% PEG-1500 (Hampton Research), and 7.5 mM $CaCl_2$ for approximately 30 s, prior to being flash frozen at 100 K in the Stanford Synchrotron Radiation Source (SSRL) beamline 9-2 cryostream. A total of 307 60-s, 0.3° wide dezingered images were collected at a crystal to detector distance 150 mm on SSRL beamline 9-2 using a Quantum-4 detector (Area Detector Systems Corp., San Diego, CA). Fourteen counts were subtracted from each image to reduce the pedestal value to six counts. This gives a more realistic approximation of the white noise inherent to CCD detectors. The adjustment improves the calculated values of I/σ. The images were then processed with X-GEN (*17*, *18*; Molecular Simulations Inc., San Diego, CA).

Crystallographic Structure Determination and Refinement. Des-GLA-factor Xaβ structures from the factor Xa/DX-9065a (PDB entry 1FAX) and factor Xa/FX-2212a (PDB entry 1XKA) were used as starting models for the refinement. The factor Xa/DX-9065a structure has the same space group and approximately the same unit cell parameters as our crystals (*8*). The factor Xa/FX-2212a structure (*9*) was solved to higher resolution. However, the protein used by Kamata et al. (*9*) included the first EGF domain of factor Xa, which was apparently missing from our own construct (Table 1). Furthermore, the larger unit cell for 1XKA indicates that the structure would not match our X-ray data. We took the factor Xa/FX-2212a coordinates as our starting model and then deleted the following groups: the first EGF domain, three C-terminal residues from the light chain, one C-terminal residue from the heavy chain, and all ligands except the calcium. These coordinates were then superimposed upon the factor Xa/DX-9065a structure and used for direct replacement. The initial refinement was performed using a series of simulated annealing runs in X-PLOR 3.1 (*19*). Initial starting temperatures were 2000 K using a 8.0−3.0 Å resolution cutoff. The high-resolution cutoff was extended to 2.3 Å, prior to fitting the inhibitor. The programs O (*20*) and XtalView (*21*) were used to refit the structure and add waters. The final refinement was done using 22 885 reflections between 8 and 1.92 Å, with a 2.0 $I/\sigma(I)$ cutoff. The final structure contains factor Xa light-chain residues L87-L138 [Swiss-Pro numbering (*22*)], heavy chain residues 16−244 [chymotrypsin numbering system (*23*)], ZK-807834, a calcium ion, a chloride ion, six glycerol molecules, and 163 waters.

RESULTS

Protein Purification, Characterization, and Crystallization. Seventeen major peaks were detected using anion-exchange chromatography to separate the partial chymotrypsin digestion of factor Xaβ (Figure 1). The molecular weights of the first five major peaks (labeled A1, A2, B1, B2, and C, Figure 1) were between 37 374 and 38 063, and the isoelectric points

Table 2: X-ray Diffraction Data and Refinement Statistics

data set	
space group	$P2_12_12_1$
wavelength (Å)	1.033
unit dimensions	
A (Å)	55.77
B (Å)	71.96
C (Å)	80.23
reflections	25 262
resolution range (Å)	
high	1.92 (1.92)[a]
low	26.1 (2.04)
completeness (%)	99.7 (99.9)
redundancy	3.6 (3.7)
R_{sym}[b]	0.054 (0.260)
mean I/σ (I)	14.1 (2.3)
refinement	
resolution (Å)	8.0−1.92
no. of reflections	
input	24 059
used ($F > 2\sigma$)	22 885
R factor	0.196
R_{free}	0.256
no. of solvent molecules	163
no. of glycerol molecules +1 Ca^{2+} and 1 Cl^-	6
RMS deviation from ideal bond length (Å)	0.011
RMS deviation from ideal bond angles (deg)	1.98

[a] Statistics for the highest resolution shell of data are shown in parentheses. [b] $R_{sym} = \sum|I - \langle I\rangle|/\sum I$.

of these peaks ran between 7.74 and 6.15 (Table 1). The results indicate that these five fractions all contained variants of des-GLA-factor Xaβ. The likely protein sequences of each peak were deduced using the ProtParam tool (*24*) to analyze the data (Table 1). The sequences differed from each other at the C-termini of both the light and heavy chains. The light-chain appeared to have three different C-termini: residues L138−L142 (ERRKR), residues L138−L141 (ERRK), or L138−L140 (ERR). The heavy chain had two possible C-termini: residues 244−249 (TRGLPK) or 244−245 (TR). The last residues seen in the crystal structure in the light chain is Glu-L138 and in the heavy chain, it is Thr244. This suggests that peak B2 has the closest sequence to that seen in the crystal structure. Following the protocol of Kamata et al. (*9*), fractions B1 and B2 were pooled together and used for crystallization. The yields for the combined B1 and B2 fractions were from 5 to 8%.

Crystals were grown from a solution of des-GLA-factor Xaβ with a 3-fold molar excess of *N*-[2-[5-[amino(imino)-methyl]-2-hydroxyphenoxy]-3,5-difluoro- 6-[3-(4,5-dihydro-1-methyl-1H-imidazol-2-yl)phenoxy]pyridin-4-yl]-*N*-methylglycine (ZK-807834). The crystals grew as clusters of thick needles and had the space group of $P2_12_12_1$. The unit cell dimensions were $a = 55.77$ Å, $b = 71.96$ Å, and $c = 80.23$ Å (Table 2).

The molecular weight of factor Xa obtained from a dissolved crystal of the protein/inhibitor complex was 33 243 ± 35. This indicates that the protein had undergone autolysis. Autolysis was also observed in the first published factor Xa structure (*23*). The observed molecular weight for our protein of 33 243 is consistent with a shortened light-chain consisting of just the EGF2 domain, residues Lys-L87 to Lys-L141, and a heavy chain from residue Ile16 to Lys249 (Table 1). The electron density for the factor Xa/ZK-807834 complex indicates that the first residue in the light chain is Lys-L87 and no electron density was observed for the EGF1 domain. It is worth noting that the protein/inhibitor solution was stored for several months at 4 °C, and it took 2−3 months to form the first crystals of factor Xa/ZK-807834. Subsequent crystals formed in only 2 weeks. Mass spectrometry of this solution revealed a complex mixture that included peaks with mass of 33 000. In subsequent work with additional inhibitors, there has been a large variation in the rate of crystal formation, from two weeks to not at all (unpublished results). These results suggest that the slow step in crystallizing the fresh solution was the autolysis of factor Xa in the presence of the potent inhibitor ZK-807834.

Crystal Structure. The crystal structure of the factor Xa/ZK-807834 complex was refined at 1.92 Å with an *R* factor of 19.6% and an R_{free} of 25.6% (Table 2; PDB entry 1FJS). The conformation of the inhibitor is clearly defined by the electron density (Figure 2). The major contacts between ZK-807834 and the protein are shown in Figure 3. ZK-807834 adopts an L-shaped conformation in factor Xa (Figures 4 and 5) similar to what was found for DX-9065a (*8*) and FX-2212a (*9*). Many potent factor Xa inhibitors share the same overall architecture as these compounds: an arylamidine connected by a linker to a second basic group.

The benzamidine of ZK-807834 fits into the S1 pocket (Figure 4). This group shall be referred to as the proximal ring. The benzamidine occupies the same position as the putative binding site of Arg323 of prothrombin, the normal substrate. The amidine forms a salt bridge to Asp189 at the bottom of the S1 pocket. Four hydrogen bonds reinforce the salt bridge: two to the carboxyl of Asp189 (2.7 Å and 3.0 Å), one to the carbonyl of Gly218 (3.1 Å), and one to a water molecule (no. 605, 2.9 Å), which is hydrogen bonded to the carbonyl of Ile227 (2.9 Å). The 2-hydroxy on the proximal phenyl ring makes a short hydrogen bond to the hydroxy of catalytic triad Ser195 (2.4 Å). The ionization of the 2-hydroxy group contributes to the short distance (the crystal were grown at pH 8.0 and this hydroxy has a pK_a of 6.82; J. Dallas, unpublished data.)

The central pyridine ring of ZK-807834 connects the two positively charged groups. It is positioned between the Trp215−Gly216 peptide bond and Gln192. The pyridine nitrogen is 3.7 Å from the amide nitrogen of Gly216, and the fluorine on the proximal side of the pyridine ring is in close contact with the side-chain amide group of Gln192 (2.9 Å). The sarcosine at position 4 on the pyridine ring has relatively weak electron density and is partially disordered (Figure 2). It has no direct contacts with factor Xa. One of the carboxyl oxygens of the sarcosine makes a hydrogen bond to a water molecule (no. 712, 2.7 Å), which is hydrogen bonded to the amide nitrogen of Gly218 (2.9 Å) and the carboxyl oxygen of Gly216 (3.1 Å).

The second positively charged group in ZK-807834 is the 1-methyl-2(1*H*)-imidazoline attached to a second phenoxy moiety. This group, which fits snugly into the S4 pocket, will be referred to as the distal ring. The phenoxy group lies across the indole ring of Trp215 (4.2 Å) and its edges contact the two flanking aromatic residues Tyr99 (4.0 Å) and Phe174 (3.7 Å). The methyl of the 1-methyl-2-(2*H*)-imidazoline is positioned above the indole ring of Trp215 in the bottom of the S4 pocket (3.2 Å to Cδ2 in the indole ring). The positive

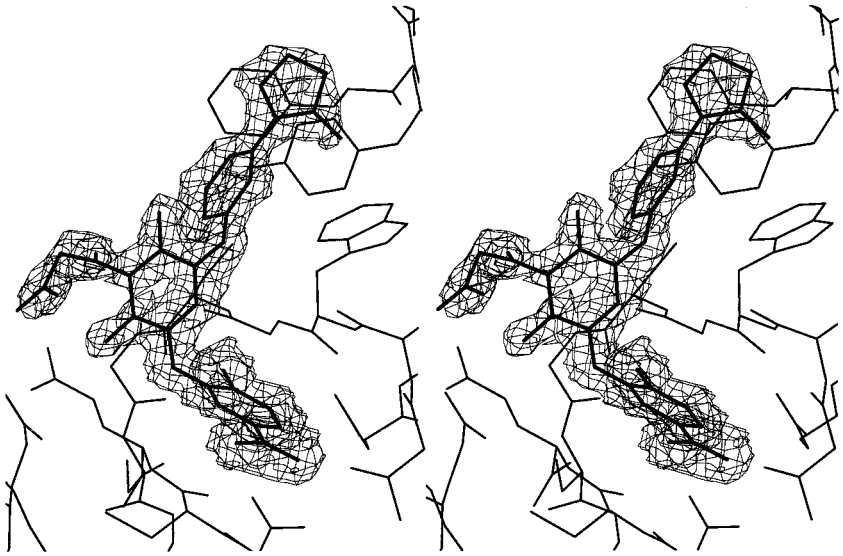

FIGURE 2: Divergent stereoview of the electron density around ZK-807834 in factor Xa. The $2F_o - F_c$ electron density map is displayed at 1.0σ. This figure was produced using the Blob option in XtalView (*21*), with minor editing with Adobe Photoshot.

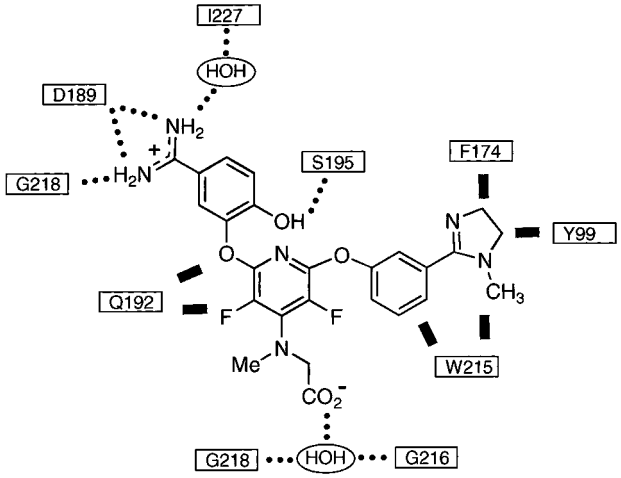

FIGURE 3: Structure of ZK-807834 showing with its major contacts with factor Xa. Hydrogen bonds are shown with dotted lines. Close contacts are shown with thick lines.

charge of the imidazoline has electrostatic interactions with the carbonyl oxygens of Lys96, Glu97, and Thr98, similar to what was found in the S4 pockets of the other factor Xa complexes (*8*, *9*). It is noteworthy that imidazoline does not form a salt bridge to any acidic residues in factor Xa. The closest negatively charged groups are the carboxyls on Glu97 (5.0 Å) and Glu217 (7.5 Å). The entire distal arm of ZK-807834 shows good shape complementarity to the S4 pocket (Figure 5A).

DISCUSSION

ZK-807834 is a potent selective inhibitor of factor Xa. Its bound conformation is similar to the published structures of two other factor Xa inhibitors: DX-9065a (*8*) and FX-2212a (*9*). Yet, ZK-807834 is at least 100 times more potent than either compound and shows >2500-fold selectivity for factor Xa vs trypsin. To understand the enhanced selectivity of ZK-807834, we must also consider how this compound interacts with trypsin. Unfortunately, there is no structural data for a trypsin/ZK-807834 complex. There is, however, extensive data on the structure activity relationships for homologous

Table 3: Binding Constants and Selectivity Data for Factor Xa Inhibitors

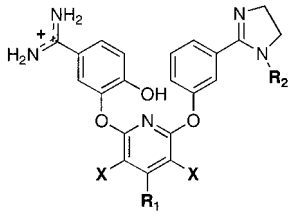

compds	X	R_1	R_2	factor Xa K_I (nM)	trypsin K_I (nM)	trypsin/ factor Xa selectivity
IV	H	CO_2^-	H	85	1400	17
V	F	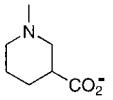	CH_3	0.11	170	1500
ZK-807834	F	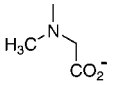	CH_3	0.11	280	2500

inhibitors in both trypsin and factor Xa (*13*, *14*). Furthermore, there are published crystal structures for several of these compounds bound to trypsin (*12*). In particular, the trypsin structures of compounds **IV** and **V** (Figure 6) show that closely related inhibitors can adopt different conformations in trypsin (compound numbering is from ref *12*). The differences in the bound conformations provide important clues to selectivity of these compounds. The results indicate that three distinct functional groups modulate the selectivity of these compounds: the 2-hydroxy on the proximal benzamidine ring, substitutions at the 3, 4, and 5 positions on the central pyridine ring, and the distal 1-methyl-2(1*H*)-imidazoline-phenoxy ring system.

Compound **V** is structurally similar to ZK-807834, and the two inhibitors have similar biochemical profiles (Table 3). Figure 6A shows the crystal structure of compound **V** bound to trypsin [PDB entry 1QB1 (*12*)]. This structure demonstrates that potent compounds in this series can adopt the same conformation in both trypsin and factor Xa. The

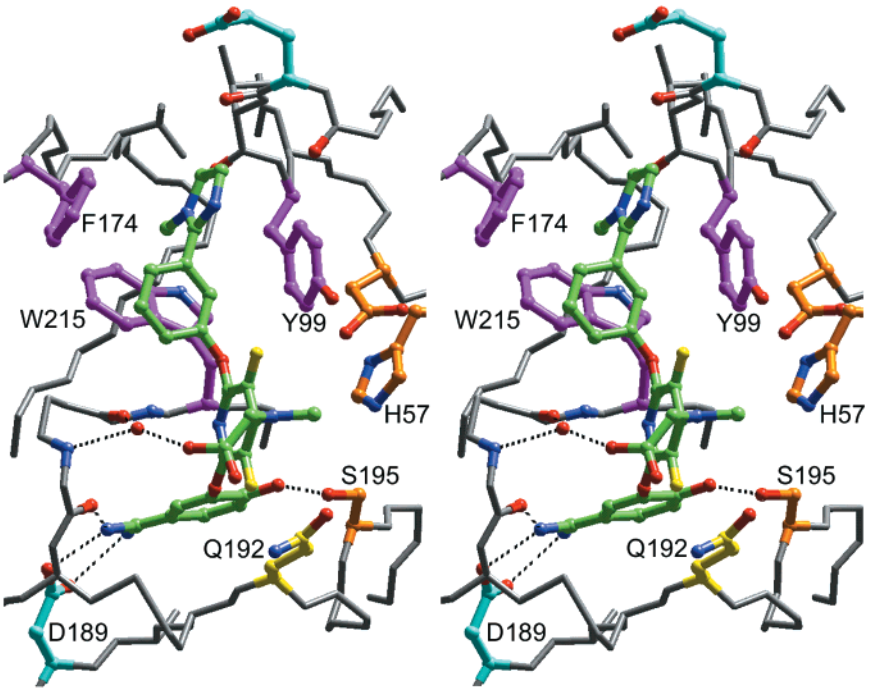

FIGURE 4: Divergent stereoview of ZK-807834 bound in factor Xa. The carbon atoms of the inhibitor are colored green. Carbon atoms of specific residues have been colored. Asp189 at the bottom of the S1 pocket and Glu97 in the S4 pocket are light blue. The catalytic triad Ser195, His57, and Asp102 are orange. Residues that form the S4 pocket, Tyr99, Phe174, and Trp215 are magenta. Hydrogen bonds are depicted as dashed lines.

2-hydroxy of **V** forms a hydrogen bond to Ser195 in trypsin (3.0 Å). The increased length of this hydrogen bond compared to the ZK-807834/factor Xa complex (2.4 Å) may reflect the more acidic conditions used in crystal growth (*12*). There are also some minor differences in the packing of the pyridine and imidazoline rings. The active site in factor Xa is lined with bulky constituents that alter the tilt of the two rings (Figure 5). The trypsin/**V** structure demonstrates that steric interactions do not interfere with the binding of these inhibitors to trypsin. Therefore, the selectivity of these inhibitors must stem from more optimal interactions with factor Xa than with trypsin.

Figure 6B compares the factor Xa/ZK-807834 complex to the trypsin bound structure of a second inhibitor in this series, compound **IV** [PDB entry 1QBN (*12*)]. Compound **IV** has different constituents than ZK-807834 at the 3, 4, and 5 positions of the central ring and the methyl group is absent from the distal imidazoline group. Table 3 shows that these changes result in a considerable loss in potency and selectivity. There are also measurable changes in the way the inhibitor binds to trypsin (Figures 5 and 6). In our experience, this second conformation frequently corresponds to reduced affinity for factor Xa (*12* and unpublished data). A detailed comparison of this structure to the factor Xa/ZK-807834 complex reveals many of the interactions that contribute to the selectivity of ZK-807834. The discussion starts with the interactions in the S1 pocket.

The crystal structures of factor Xa inhibitors in this series all show a salt bridge between the proximal benzamidine and Asp189 in the S1 pocket. The S1 pocket in both trypsin and factor Xa is designed to bind basic amino acids and there are very few structural differences between the proteins in this cavity. For the benzamidine-based inhibitors, the addition of the 2-hydroxy to the phenyl ring increases factor Xa affinity by 8−70-fold and in trypsin by only 1.3−2.5-fold (*13*, *14*, and unpublished data). This modification provides the single largest enhancement in selectivity for compounds that use the pyridine template. In factor Xa, the 2-hydroxy forms a short hydrogen bond with the active site Ser195 (2.4 Å). The structure of the compounds in trypsin show that sometimes this hydrogen bond forms (3.0 Å for **V**, Figure 6A) and sometimes it does not (3.6 Å for **IV**, Figure 6B). Thus, an important question is why the formation of the hydrogen bond is so energetically favorable in the factor Xa/ZK-807834 complex, but seemingly has little effect on trypsin binding.

A comparison of the trypsin and factor Xa structures indicates there are three potential explanations for the differences in hydrogen bond formation. First, there is a substitution in factor Xa of an alanine for Ser190 in trypsin. [Like factor Xa, trypsin is numbered using the chymotrypsin scheme (*25*).] The Ser190→Ala is the only substitution that directly contacts the inhibitor in the S1 pocket. However, the Ser190 Oγ is 7.4 Å from the Oγ of Ser195 in trypsin, and the substitution has little effect on the position of the benzamidine group of compound **V** (Figure 6A). Ser190 in trypsin may exert an indirect electrostatic effect on the 2-hydroxy through the benzamidine ring of the inhibitor.

The second difference between trypsin and factor Xa involves the active-site triad: Ser195, His57, and Asp102. In factor Xa, His57 is protected from the solvent by three residues: Tyr99, Tyr60, and Gln61. These three residues fill the S2 binding pocket; a feature found in the active site of other serine proteases. In trypsin, the loop containing Lys60 and Ser61 folds away from S2, and there is a Tyr to Leu substitution at residue 99. These substitutions in trypsin expose His57 to the solvent. This in turn may affect the electrostatic interactions with Ser195 and have an indirect effect on the formation of hydrogen bonds to the inhibitors.

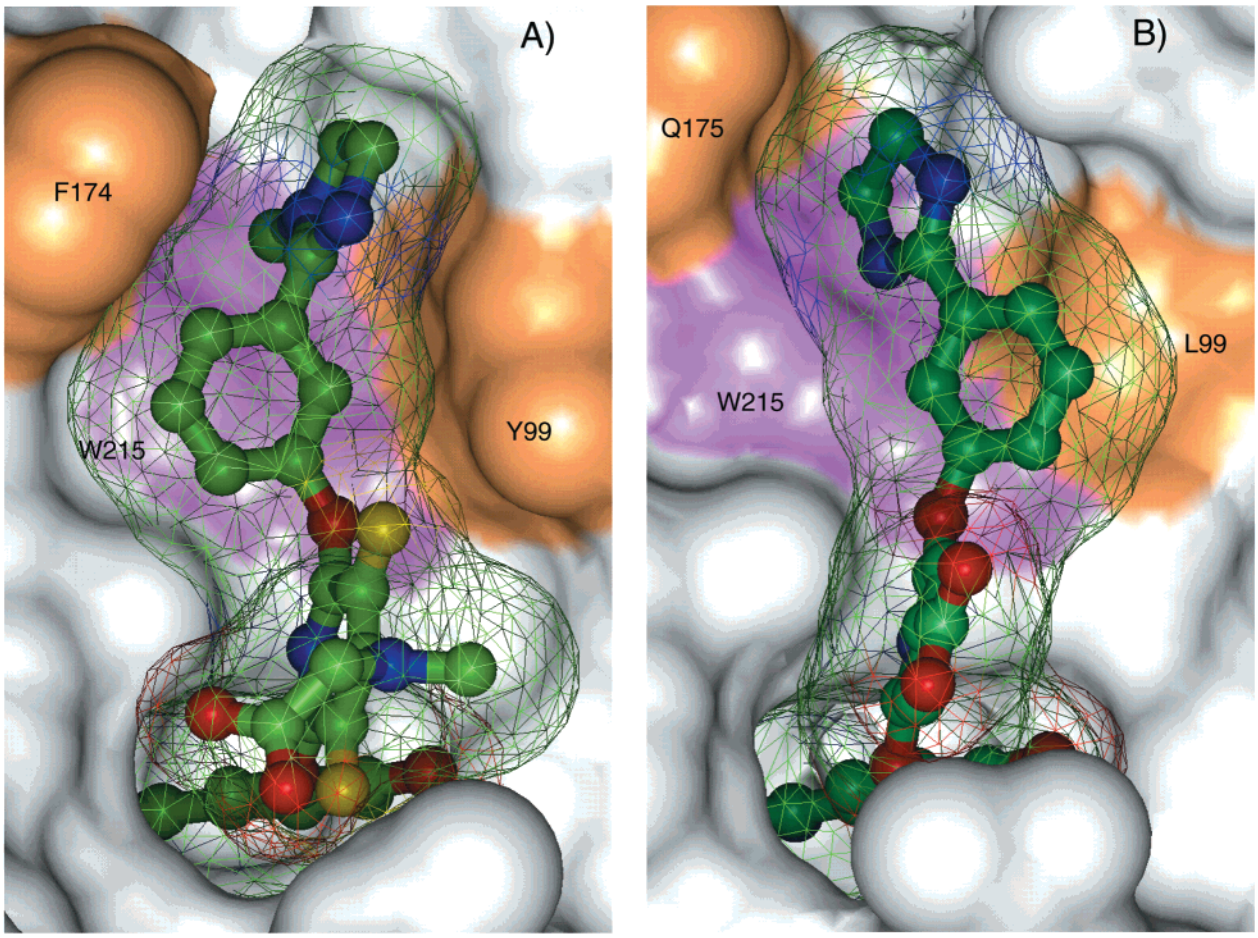

FIGURE 5: Connelly surfaces of (A) ZK-807834 bound to factor Xa and (B) compound **IV** bound to trypsin. The proteins are shown with a white solid surface and the surface of the conserved Trp215 shown in light purple. The surfaces of residues Tyr99 and Phe174 in factor Xa are shown in orange. The corresponding residues in trypsin are Leu99 and Gln175. The surfaces for the two inhibitors are portrayed as wireframe that is color-coded by the individual atoms. Figure was prepared using insightII (Molecular Simulations Inc., San Diego, CA).

Finally, there are important differences in the second shell of residues that surround the active site. In factor Xa, there are nine charged residues flanking the active site: Lys96, Glu97, Arg143, Glu146, Lys147, Arg150, Glu217, Arg222, and Lys224 (net charge of +3). Only one charged residue flanks the active site in bovine trypsin, Lys224 (net charge of +2). These charges may influence the interactions between the 2-hydroxy and Ser195. However, long-range electrostatic interactions are attenuated by intervening solvent and it is difficult to predict how these charged residues influence the binding of inhibitors.

The central pyridine ring that connects the proximal and distal ring is more rigid than the corresponding linkers in both DX-9065a (*8*) and FX-2212a (*9*). It is likely that the rigidity of the ring contributes to the potency of ZK-807834 by limiting the entropic losses during binding. Substitutions on the central ring provide minor enhancements to the selectivity of these compounds (*13*, *14*). Fluorine substitutions at positions 3 and 5 of the pyridine ring result in a 2−5-fold increase in factor Xa affinity, but they do not alter the affinity for trypsin. The fluorines may limit the rotation around the bonds connecting the pyridine to the two phenyl ethers. They may also have long-range electrostatic interactions with the second shell of residues that surround the active site (discussed above). The sarcosine forms a water-mediated hydrogen bond with Gly216 and Gly218 in factor Xa, but it has no direct contact with the protein. The sarcosine moiety also contributes to the >10 000-fold selectivity of ZK-807834 for factor Xa verses thrombin (*13*). The negatively charged carboxylic acid is believed to have a repulsive interaction with Glu192 of thrombin, which is located at the top of the S1 pocket. Both factor Xa and trypsin have a glutamine in this position. This is the only residue that maintains close contact with the central ring.

The S4 pocket is deeper and more hydrophobic in factor Xa than in trypsin (Figure 5). These changes arise from the substitutions of Leu99→Tyr and Gln175→Phe174 in factor Xa. Tyr99 and Phe174 create a groove about 5 Å wide and 4 Å deep. The Tyr99 substitution is also significant because it precludes access to the S2 pocket in factor Xa. In addition, two negatively charged residues, Glu97 and Glu217, flank the S4 pocket in factor Xa. The corresponding residues in trypsin are Asn97 and Ser217. Presumably, these substitutions add specificity to the binding of the S4 pocket in factor Xa. The S4 pocket in trypsin is broader and lined with hydrophilic residues on the left side of the channel (Gln175 and Ser217 in Figure 6A).

Crystal structures of the inhibitors complexed with either factor Xa or trypsin all show positively charged groups in close contact with the indole ring of Trp215 (*8*−*10*, *12*, and unpublished data). The average interatomic distance of the closest contact is 3.6 ± 0.25 Å. The trypsin structures display some variations on how the positively charged ring is connected back to the central ring. Most linker groups are

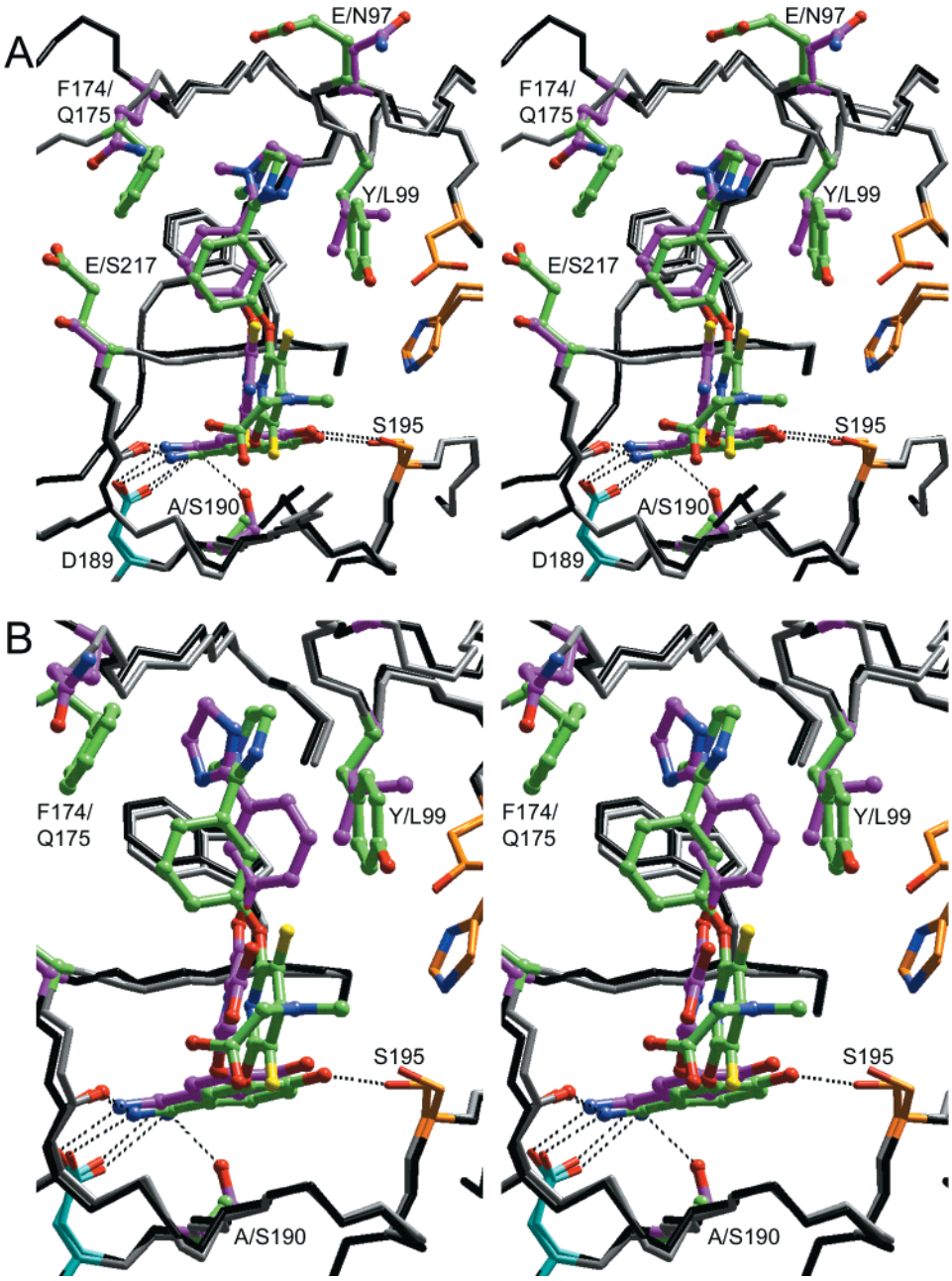

FIGURE 6: Divergent stereoview of the superposition of the factor Xa/ZK-807834 complex with (A) bovine trypsin/**V** (PDB entry 1QB1) and (B) bovine trypsin/**IV** (PDB entry 1QBN). The carbon atoms in ZK-807834 are green. The corresponding atoms in compounds **IV** and **V** are magenta. The same color scheme is used for several critical amino acid substitutions: green carbon atoms in factor Xa and magenta in trypsin. The catalytic triad residues (Ser195, His57, and Asp102) in both structures are colored orange and the Asp189 has light-blue carbon atoms. The remaining atoms are colored gray in factor Xa and black in trypsin. The piperidine ring in compound **V** (group R1 in Table 3) was deleted since its position could not be determined from the electron density. For panel B, part of the S1 pocket had been removed to facilitate viewing.

in van der Waals contact with Leu99 (compound **IV**, Figure 5B). This type of binding is excluded in factor Xa because the linker would overlap with Tyr99 (Figure 5A). A few inhibitors in trypsin have an aromatic ring that is stacked on top of Trp215. In the trypsin/**V** complex, the distal phenoxy has significant hydrophobic contacts with the ring system of Trp215 (Figure 6A). This interaction shifts the linker by several angstroms, positioning it to fit snugly into the S4 pocket of factor Xa. In our experience, compounds that demonstrate this ring stacking with Trp215, in either trypsin or factor Xa, all have at least a 1000-fold selectivity for factor Xa verses trypsin. Clearly, multiple modifications contribute to the selectivity of these compounds, but this interaction appears to make an important contribution.

Finally, the 1-methyl substitution on the distal imidazoline ring improves the selectivity of these compounds in this series by about 7-fold. Part of this increase probably stems from changes in desolvation energy; it is more favorable to bring the methyl group into a hydrophobic S4 pocket of factor Xa. However, the addition of the methyl group also results in an important change in the geometry of the molecule. The distal arms of compounds **V** and **IV** are identical except for this additional methyl on the imidazoline group in **V**. The methyl group of **V** allows the imidazoline

group to retain a close contact with Trp215 in trypsin (3.2 Å). In the trypsin/**IV** structure, the imidazoline ring must shift by 1 Å to maintain close contact with the tryptophan (Figure 6B). This displacement of the imidazoline ring forces the connecting phenoxy group away from Trp215 and toward Leu99 (Figure 5B). The same phenoxy ring in compound **V** stacks directly against Trp215 (Figure 6A). Only the latter conformation is compatible with binding to factor Xa and the activity measurements confirm that this modification is important (Table 3).

CONCLUSIONS

Comparisons of the factor Xa and trypsin structures provide explanations for why the modifications of the proximal and distal rings of ZK-807834 are important to the binding properties of the inhibitors. The results highlight two important interactions: the formation of a hydrogen bond to Ser195 and aromatic ring stacking with Trp215. The central pyridine ring provides a rigid base of support for the proximal and distal arms of the inhibitor. It is likely that this rigidity increases potency by minimizing the entropy losses during binding. The knowledge gained from the various crystal structures continues to be applied to rational design of selective serine protease inhibitors.

ACKNOWLEDGMENT

We would like to thank Bill Dole, Michael Morrissey, and John Morser for the support of this work. We thank Tim Slattery and Sara Biancalana for their help with the mass and isoelectric point determinations. Amy Liang determined the inhibition constants for all of the compounds. Furthermore, we thank Meg McCarrick, and Ken Shaw for their insights and their editorial assistance in preparing the manuscript.

REFERENCES

1. Davie, E. W., Fujikawa, K., and Kisiel, W., (1991) *Biochemistry 30*, 10363−10370.
2. Mann, K. G. (1999) *Thromb. Haemost. 82*, 165−174.
3. Kung, C., Hayes, E., and Mann, K. G. (1994) *J. Biol. Chem. 269*, 25838−25848.
4. Prager, N. A., Abendschein, D. R., McKenzie, C. R., and Eisenberg, P. R. (1995) *Circulation 92*, 962−967.
5. McKenzie, C. R., Abendschein, D. R., and Eisenberg, P. R. (1996) *Arterioscler. Thromb. Vasc. Biol. 16*, 1285−1291.
6. Jones, K. C., and Mann, K. G. (1994) *J. Biol. Chem. 269*, 23367−23373.
7. Nicolini, F. A., Lee, P., Malycky, J. L., Lefkovits, J., Kottke-Marchant, K., Plow, E. F., and Topol, E. J. (1996) *Blood Coagul. Fibrinol. 7*, 39−48.
8. Brandstetter, H., Kuhne, A., Bode, W., Huber, R., von der Saal, W., Wirthensohn, K., and Engh, R. A. (1996) *J. Biol. Chem. 271*, 29988−29992.
9. Kamata, K., Kawamoto, H., Honma, T., Iwama, T., and Kim, S.-H. (1998) *Proc. Natl. Acad. Sci. U.S.A. 95*, 6630−6635.
10. Wei, A., Alexander, R., Duke, J., Ross, H., Rosenfeld, S. A., and Chang, C.-H. (1998) *J. Mol. Biol. 283*, 147−154.
11. Renatus, M., Bode, W., Huber, R., Stürzebecher, J., and Stubbs, M. T. (1998) *J. Med Chem. 41*, 5445−5456.
12. Whitlow, M., Arnaiz, D. O., Buckman, B. O., Daves, D. D., Griedel, B., Guilford, W. J., Koovakkat, S. K., Liang, A., Mohan, R., Phillips, G. B., Seto, M., Shaw, K. J., Xu, W., Zhao, Z., Light, D. R., and Morrissey, M. M. (1999) *Acta Crystallogr., Sect. D 55*, 1395−1404.
13. Phillips, G. B., Buckman, B. O., Davey, D. D., Eagen, K. A., Guilford, W. J., Hinchman, J., Ho, E., Koovakkat, S., Liang, A., Light, D. R., Mohan, R., Ng, H. P., Post, J., Smith, D., Shaw, K. J., Subramanyam, B., Sullivan, M. E., Trinh, L., Vergona, R., Walters, J., White, K., Whitlow, M., Wu, S., Xu W., and Morrissey, M. M. (1998) *J. Med. Chem. 41*, 3557−3562.
14. Phillips, G., Davey, D. D., Eagen, K. A., Koovakkat, S. K., Liang, A., Ng, H. P., Pinkerton, M., Trinh, L., Whitlow, M., Beatty, A. M., and Morrissey, M. M. (1999) *J. Med. Chem. 42*, 1749−1756.
15. Abendschein, D. R., Baum, P. K., Martin, D. J., Vergona, R., Post, J., Rumennik, G., Sullivan, M. E., Eisenberg, P. R., and Light, D. R. (2000) *J. Cardiovasc. Pharmacol. 35*, 796−805.
16. Jancarik, J., and Kim, S.-H. (1991) *J. Appl. Crystallogr. 24*, 409−411.
17. Howard, A. J., Gilliland, G. L., Finzel, B. C., Poulos, T. L., Ohlendorf, D. H., and Salemme, F. R. (1987) *J. Appl. Crystallogr. 20*, 383−387.
18. Molecular Simulation Inc. X-GEN product information (April 21, 2000) http://www.msi.com/life/products/cerius2/modules/c2xgen.html.
19. Brünger, A. (1993) *X-PLOR: A System for X-ray Crystallography and NMR*, Version 3.1, New Haven, Yale University Press.
20. Jones, T. A., Zou, J. Y., Cowan, S. W., and Kjeldgaard, M. (1991) *Acta Crystallogr., Sect. A 47*, 110−119.
21. McGee, D. E. (1992) *J. Mol. Graphics 10*, 44−46.
22. NiceProt View of SWISS−PROT: P00742 (April 21, 2000) http://www.expasy.ch/cgi-bin/niceprot.pl?P00742.
23. Padmanabhan, K., Padmanabhan, K. P., Tulinsky, A., Park, C. H., Bode, W., Huber, R., Blankenship, D. T., Cardin, A. D., and Kisiel, W. (1993) *J. Mol. Biol. 232*, 947−966.
24. ExPASy - Protparam tool (April 21, 2000) http://www.expasy.ch/tools/protparam.html.
25. Bode, W., Turk D., and Karshikov, A. (1992) *Protein Sci. 1*, 426−471.

BI001477Q